Available online at www.sciencedirect.com

ScienceDirect

Procedia Structural Integrity 26 (2020) 11–19

Structural Integrity Procedia

www.elsevier.com/locate/procedia

The 1st Mediterranean Conference on Fracture and Structural Integrity, MedFract1

Post welding heat treatment improving mechanical properties on Ti-6Al-4V

P. Ferro[a,*], F. Berto[b], F. Bonollo[a], L. Romanin[a], G. Salemi[c]

[a] *Department of Engineering and Management, University of Padova, Stradella San Nicola 3, 36100 Vicenza (Italy)*
[b] *NTNU, Department of Engineering Design and Materials, Richard Birkelands vei 2b, 7491, Trondheim (Norway)*
[c] *Dallara, Via Provinciale, 33 43040 Varano de' Melegari, Parma (Italy)*

Abstract

Ti-6Al-4V can be easily welded by tungsten inert gas (TIG) welding process. However, the parent material properties tend to worsen because of microstructural changes and residual stresses. Post welding heat treatments (PWHT) are used to restore the mechanical properties of the joints. In this work, automotive components made out of Ti-6Al-4V are welded by TIG process. Although the as-welded joints showed e reasonable static strength, the strain at failure resulted quite low so that a toughness improvement via post welding heat treatment was required. This contribution summarizes the preliminary results obtained by PWHT on both butt- and overlap-welded joints made out of titanium alloy (grade 5). Different heat treatment (HT) recipes were tested and results were showed in terms of stress-strains curves as well as microstructure and microhardness profiles. It is found that, with reference to overlap joints, a stress-relieving HT optimizes both the mechanical properties and toughness. A partial solution HT followed by ageing is required to increase significantly the static strength of butt-welded joints, unfortunately without toughness improvement.

Keywords: Welding; Titanium Alloy; Pahse Transformations; Mechanical Properties, Post Welding Heat Treatment

* Corresponding author.
E-mail address: paolo.ferro@unipd.it

2452-3216
10.1016/j.prostr.2020.06.003

1. Introduction

Ti-6Al-4V is widely used in lightweight design because of its high specific strength compared to other alloys, and excellent high-temperature properties (Boyer, 1996; Picu and Majorell, 2002). Another advantage is that it is easily weldable by conventional processes like tungsten inert gas (TIG) welding (Mehdi et al., 2016). The thermal cycles induced by the heat source on fusion zone (FZ) and heat affected zone (HAZ) cause complex microstructural transformations. A considerable prior β-grain growth and a wholly or partially martensitic microstructure, affecting negatively the joints ductility, is often observed due to the rapid heating and cooling in HAZ (Sundaresan et al.,1999). Residual stresses accompany also the welding process, worsening the mechanical properties of the welded parts (Balasubramanian et al., 2009; Babu and Raman, 2006). Both residual stresses and increased dislocations density induced by fusion welding may promote a premature failure of the joints, resulting in a shortened service life (Chuan et al., 2009; Chang and Teng, 2004; Brickstad and Josefson, 1998). Post welding heat treatments (PWHT) are commonly used to stabilize microstructure, decrease the inhomogeneity of the structure and improve the mechanical properties of Ti-6Al-4V welded joints. However, the majority of the works found in literature are focused on the effects of PWHT on the metallurgical and mechanical properties of welded components obtained by high power density processes such as laser or electron beam welding (Kabir et al., 2012; Gao et al., 2013; Thomas et al., 1993). Kabir et al. (2012) studied the effects of two PWHTs (stress-relief annealing and solution heat treatment followed by aging) on the metallurgical and mechanical properties of Ti-6Al-4V welded by using a continuous wave (CW) 4-kW Nd:YAG laser welding machine. No positive effects were observed on post welding heat treated samples when compared with the mechanical properties of the as-welded joints.

As the PWHT temperature increases, residual stresses relieve faster and more effectively (Dong et al., 2014). However, the mechanical properties may worsen if the PWHT temperature is above 700 °C as the grains coarsen (Kabir et al., 2012; Thomas et al.,1993). Yan et al. (2017) studied the effect of post welding stress-relieving heat treatment (700 °C for 1h) to the static and fatigue properties of Ti-6Al-4V TIG welded joints. The results indicate that the PWHT increases the yield strength of weld metal around 2.1% and improves the low cycle tensile fatigue life significantly under fatigue loads from 750 MPa to 950 MPa by reducing residual stresses to close to 0 MPa. Such positive effects of PWHT were attributed by the authors to stress reliving only, since no microstructural variations were observed compared to the as-welded joints.

This contribute is aimed at studying the effect of different PWHTs on Ti-6Al-4V TIG welded joints mechanical properties. Starting from the results by Yan et al. (2017), stress-relieving heat treatments with two different dwell times were tested. Furthermore, partial solution and quenching heat treatments followed by 600 °C aging with three different dwell times were analyzed.

2. Materials, geometry and experiments

The chemical composition of the material under investigation is given in Table 1. The phase diagram of the alloy used to design the post welding heat treatments (PWHT) is shown in Fig. 1. Two different welding geometries were tested, butt-welded and overlap-welded joints (Fig. 2). The thickness of the welded plates was 4.2 mm (L_0 = 65 mm). The two TIG welding runs were carried out with process parameters summarized in table 2; argon was used as shielding gas. The butt-welded joints geometry as well as the testing procedure were made according to the Standard UNI EN ISO 4136. It is noted that additional fixtures were bonded at the two ends of the single lap joints in order to assure a perfect alignment of the load during the tensile test. Vickers micro-hardness profiles across the weld bead section were obtained using a load of 200 g and a dwell time of 15 s. Finally, metallographic investigation was performed by using optical microscopy (Leica DM6 M) on samples etched by the following solution: 1 to 3 mL of HF + 2 to 6 mL of HNO_3 + 100 mL of H_20.

Table 1. Chemical composition of the as-received material (wt%).

	Al	V	C	Fe	O	Z	H
Parent metal	6.1	3.89	0.25	0.17	0.15	0.013	0.003

Table 2. Welding process parameters.

Weld pass	Filler metal		Current		Volt	Speed (cm/min)
	Type class	Diameter (mm)	Type & Polarity	Ampere		
1°	ER Ti-5	3.2	DE - EN	95	14	11
2°	ER Ti-5	3.2	DE - EN	126	15	11

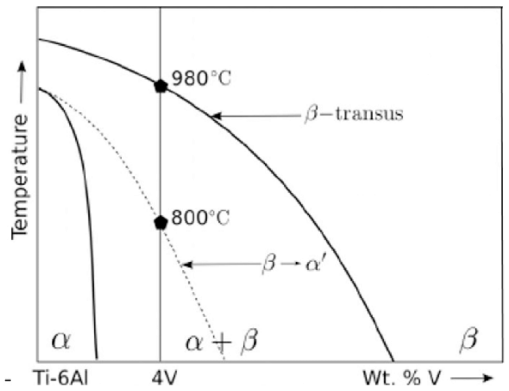

Fig. 1. Phase diagram of the alloy under investigation

Two different PWHTs were investigated, a stress-relieving heat treatment (SR) and a partial solution and quenching heat treatment followed by aging (SQA) (Fig. 3).

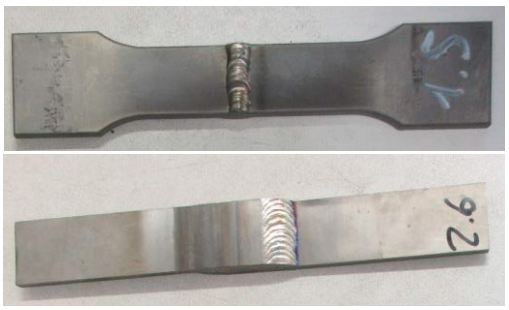

Fig. 2. Geometries of the samples for tensile tests

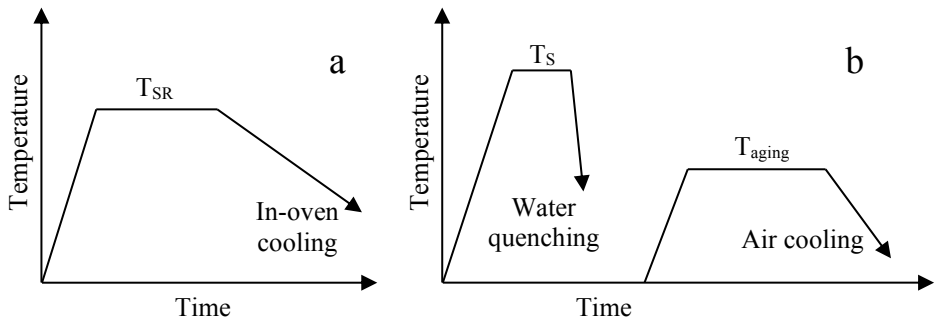

Fig. 3. Schematics of the PWHTs investigated: a) stress-relief (SR) heat treatment and b) partial solution and quenching heat treatment followed by aging (SQA)

Table 3 summarizes the PWHT temperatures and dwell times used in the experiments.

Table 3. Heat treatments parameters used in the experiments.

SR		T_{SR} (°C)		Dwell stress-relief time (h)	
	SR1	700		1	
	SR2			4	
		T_S (°C)	Dwell solution HT time (h)	T_{aging} (°C)	Dwell aging time (h)
SQA	SQA1	930	1	600	1
	SQA2	900			5
	SQA3	900			9

3. Results and discussion

3.1 Microstructure

For the sake of simplicity, only the micrographic investigation carried out on the as-welded, SR1 and SQA1 samples are reported. Fig. 4 shows the macrographs of the as-welded butt- and overlap-joints, while in Fig. 5 the microstructures of parent metal (PM), fusion zone (FZ) and heat affected zone (HAZ) of butt-welded joints after SR1 and SQA1 heat treatments are shown.

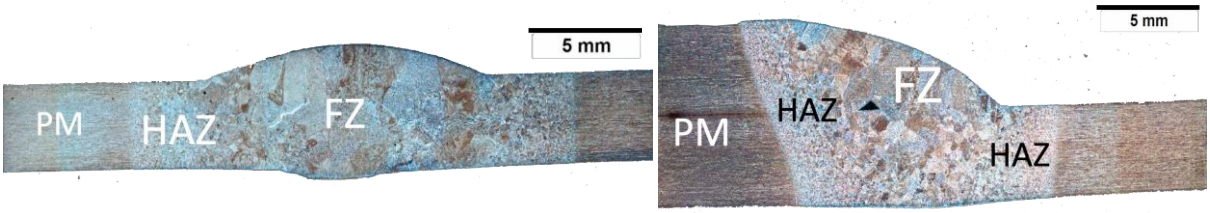

Fig. 4. Macrographs of the as-welded joints

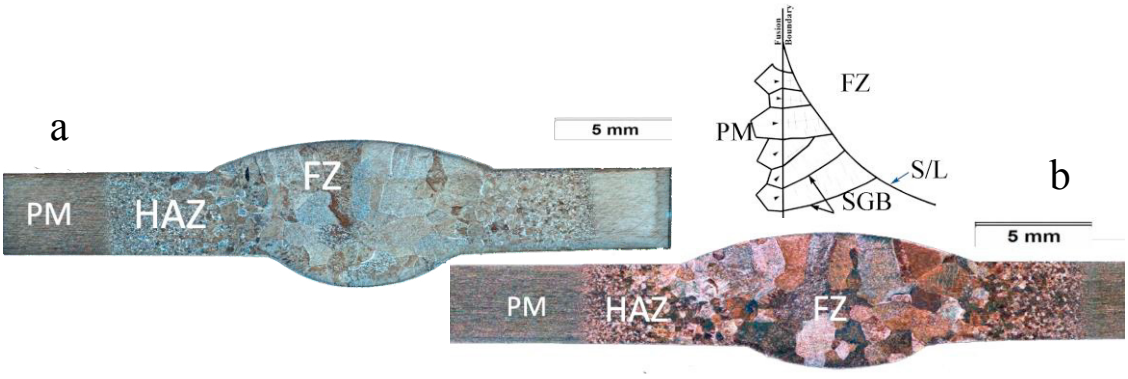

Fig. 5. Macrographs of butt-welded joints after SR1 (a) and SQA1 (b) heat treatments

In all joints the typical *epitaxial* grain growth was observed. Solidification grain boundaries (SGBs) formed starting from the original grains in PM/FZ boundary and followed the heat dissipation direction that is perpendicular to the solid/liquid interface (Fig. 5). Furthermore, it is noted a prior β-grain size increase starting from the PM and approaching the welding centre line. In a first overview of macrographs, nothing seems to change from the microstructure of as-welded and SR1 heat treated samples. Fig. 6 shows micrographs of butt-welded joints as a function of weld bead

zone and heat treatment. The average grain size (in PM) and prior β-grain size value (in FZ and HAZ) are also reported in each micrograph as well as the grain shape factor for PM microstructures only. Both heat treatments affect the shape of the elongated grain of the as-received PM by promoting an equiaxial morphology without increasing the mean size. Further, the increase of prior β-grain size from the HAZ to the FZ, induced by welding, was not significantly affected by the heat treatments tested.

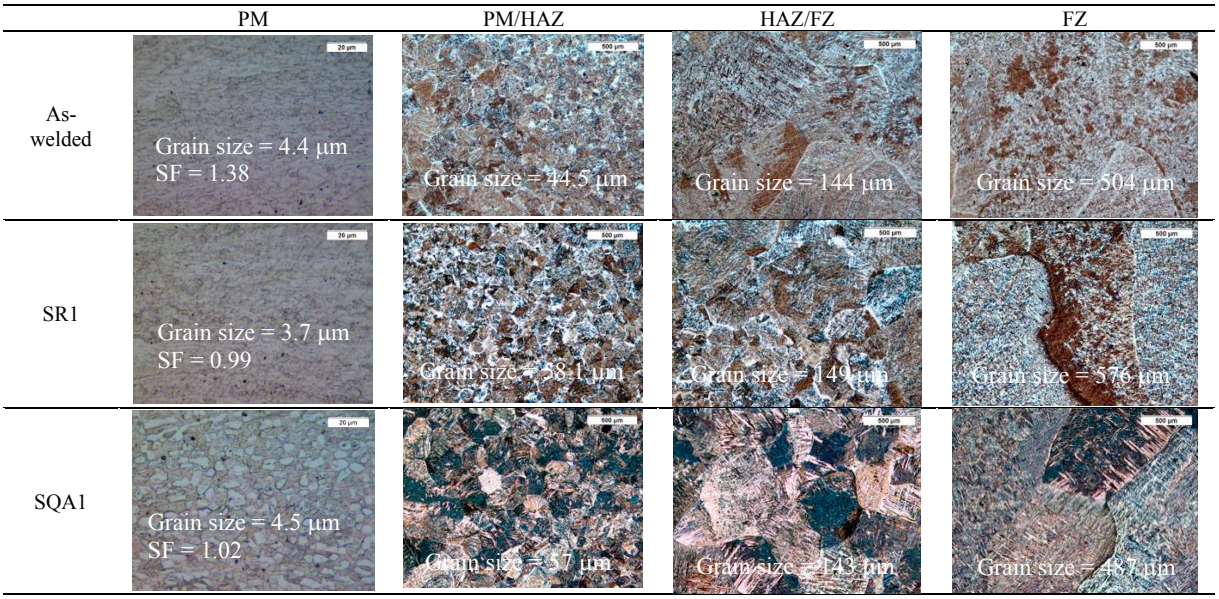

Fig. 6. Micrographs of butt-welded joints as a function of weld bead zone and heat treatment

Parent metal microstructure consists of massive α-grains decorated with a small amount of β-phase. FZ and HAZ show a sudden increase of prior β-grains. Optical micrographs of the as-welded joints FZs illustrate the dominance of acicular morphologies within the microstructure that seems to be mainly α' martensite (Gil et al., 2001; Ahmed and Rack, 1998). However, the formation of an acicular α phase, that has a similar morphology to α' phase as explained by Sundaresan et al. (1999), is not excluded. Some thin layers of diffusional α grain boundary and retained β phases (named α_{GB} and β_r respectively) are also observed. α' appears in the form of thin needles within the prior β grains.

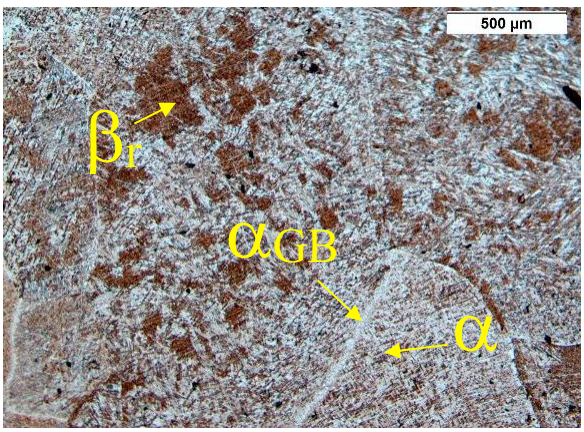

Fig. 7. FZ of as-welded overlap welded joint showing a mixture of martensitic α', diffusional α (α_{GB}) and retained β.

The microstructure of the HAZ is shown in Fig. 8 and comprises both α + β structures as well as acicular phase that seems to be α and α'. During continued cooling, α plates nucleate at the β grain boundaries and grow into the β

grains as parallel plates forming the so-called α colony. The α colonies continue to grow until they meet another α colony. With increasing cooling rate, the size of the α colonies as well as the thickness of the individual α plates becomes smaller. At higher cooling rates α plates start to nucleate also at the α colony boundaries and start to grow perpendicular to the nucleation site forming basketweave structure (Fig. 8).

The SR heat treatments didn't affect significantly the original microstructure of the joints, while great amount of coarse acicular α occurred in the FZ of SQA heat treated samples. Furthermore, martensitic α' decomposes to equilibrium α and β even if the decomposition is not completed at the aging temperature up to 600°C.

3.2 Microhardness

Fig. 9 collects the microhardness profiles as a function of the butt-welded joint condition. All of them show a quite flat shape with a little increment of the microhardness by approaching the FZ. The lowest values are measured in the as-welded joints while the biggest ones are observed in the SQA1 post heat treated samples. This is attributed to the higher amount of α' phase in the last ones, induced by the solution and quenching and only partially decomposed during the 1h aging heat treatment at 600 °C. By increasing the aging dwell time, the increased decomposition of α' reduces the hardness of the joint as shown in Fig. 9.

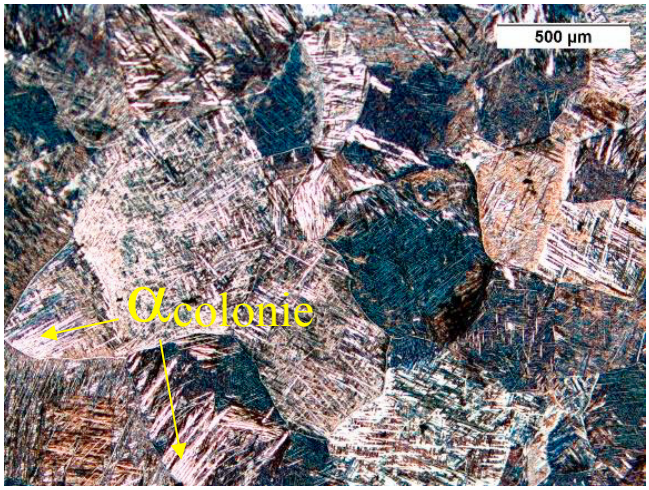

Fig. 8. HAZ of as-welded butt joint

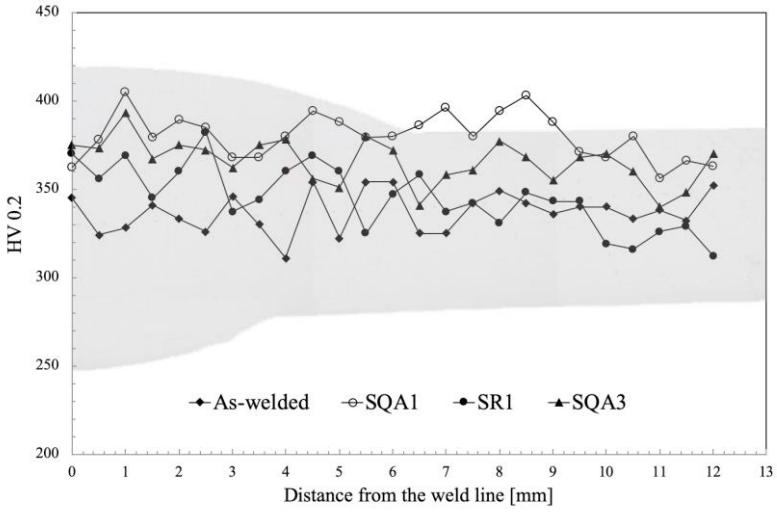

Fig. 9. Microhardness profiles

3.3 Tensile tests

For conservative reasons, only the stress-strain curves showing the minimum mechanical properties resulting for each condition, say as-welded or post welding heat treated condition, are reported in Fig. 10. For the sake of clarity, it is pointed out that, for each condition, the difference among results were restricted only to the strain at failure that is affected by geometric weld toe variations, singular residual stress fields (Ferro and Berto, 2016) and defects as well. Table 4 collects the numerical values of the yield stress (σ_y) for the butt-welded joints and the ultimate tensile stress (UTS) for the overlap joints as a function of the PWHT tested. Furthermore, minimum toughness indexes (I_T), estimated with the formula shown in the bottom of table, are reported.

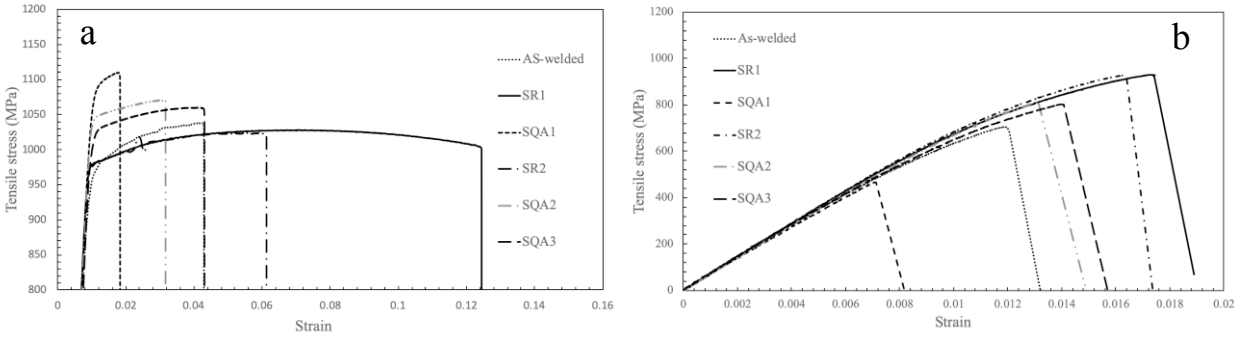

Fig. 10. Nominal stress strain curves of butt-welded (a) and overlap welded (b) joints

Table 4. Mechanical strength and minimum toughness index as a function of PWHT.

	Butt-welded joint		Overlap welded joint	
	σ_y (MPa)	I_T (mJ/mm^3) *	UTS (MPa)	I_T (mJ/mm^3) **
As welded	960	34	734	5
SR1	980	118	929	9
SR2	980	53	927	8
SQA1	1080	10	483	2
SQA2	1080	26	807	6
SQA3	1060	35	801	6

* $I_T = UTS \times \varepsilon_f$
** $I_T = (UTS \times \varepsilon_f)/2$

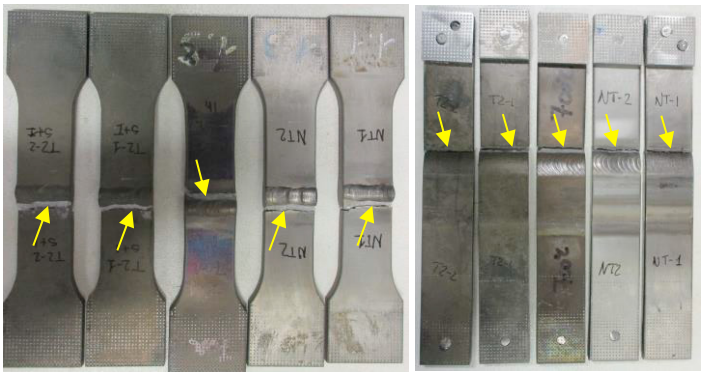

Fig. 11. Welded joints failures at the HAZ

SR heat treatments increase the yield strength of butt-weld metal around 2% that is the same improvement obtained by Yan et al. (2017) and attributed by the authors to the stress-relief effect only. The toughness increment is much more significant. A longer dwell time (SR2) doesn't affect the yield stress but reduces the toughness because of the micro-structure coarsening effect. SQA heat treatments applied to butt-welded joints increase the yield stress from 10.4% to 12.5% but the dwell time must be 9h long if at least the toughness of the as-welded joint needs to be reached. This is due to an increased amount of α' phase in the microstructure of the weld bead after quenching followed by its partial decomposition to equilibrium α and β phases according to the dwell time. Almost opposite results are obtained with regard to overlap joints. In this case the UTS increment promoted by SR1 and SR2 is about 26% followed by an increment of the toughness value, as well. The SQA1 heat treatment gave the worst results in terms of strength and ductility. On the other hand, SQA2 and SQA3 heat treatment increases the yield strength of butt-weld metal around 10%, while maintaining almost constant the joint toughness. Finally, all samples brock near the HAZ/PM interface (Fig. 11)

5. Conclusions

Metallurgical and mechanical analyses were carried out on both butt- and overlap- welded joints in the as-received and after PWHT conditions. Two PWHTs were carried out, a stress-relieving heat treatment and a partial solution and quenching heat treatment followed by aging. In the first one the oven temperature was 700 °C and the dwell time varied from 1h to 4h; in the second one, the dwell aging time at 600 °C was varied from 1h to 9h. Stress-relieved joints didn't show a significant change in the microstructure, compared to the as-welded samples and the strength increment of 2% followed by a significant toughness improvement was attribute to the residual stress reduction as confirmed by the literature. SQA heat treatments applied to butt-welded joints showed better results in terms of mechanical strength (about 11% of yield stress improvement) but no improvement in terms of toughness. It was attributed to an increase of acicular α' phase in the weld bead microstructure. The PWHTs that promoted the best mechanical properties on overlap welded joints ware the stress-relieving heat treatments with an increase of the UTS of about 26% even accompanied by a significant toughness improvement.

Acknowledgements

The authors would like to acknowledge the support provided by Giacomo Mazzacacallo to the experimets carried out in the present work. Special thanks are due also to DALLARA s.p.a. for the material supply.

References

Gil, F.J., Ginebra, M.P., Manero, J.M., Planell, J.A., 2001. Formation of α-Widmanstatten structure: effects of grain size and cooling rate on the Widmanstatten morphologies and on the mechanical properties in Ti6Al4V alloy. J. Alloys Compd. 329, 142 – 152.

Ahmed, T., Rack, H.J., 1998. Phase transformations during cooling in α+β titanium alloys. Mater. Sci. Eng. A 243, 206 – 211.

Sundaresan, S., Janaki, R.G., Madhusudhan, R.G., 1999. Microstructural refinement of weld fusion zones in alpha-beta titanium alloy using pulsed current welding. Mater. Sci. Eng. A 262, 88–100.

R. Boyer, "An overview on the use of titanium in the aerospace industry," Materials Science and Engineering: A, 213 (1996) 103-114.

R. Picu, A. Majorell, Mechanical behavior of Ti-6Al-4V at high and moderate temperatures—Part II: constitutive modeling, Materials Science and Engineering: A 326 (2002) 306-316.

B Mehdi, Riad Badji, V Ji, B Allili, D Bradai, et al.. Microstructure and residual stresses in Ti-6Al- 4V alloy pulsed and unpulsed TIG welds. Journal of Materials Processing Technology, Elsevier, 2016, 231, pp.441-448. 10.1016/j.jmatprotec.2016.01.018 . hal-01289332

M. Balasubramanian, V. Jayabalan, V. Balasubramanian, Prediction and optimization of pulsed current gas tungsten arc welding process parameters to obtain sound weld pool geometry in titanium alloy using lexicographic method, Journal of Materials Engineering and Performance 18 (2009) 871-877.

N.K. Babu, S.G.S. Raman, Influence of current pulsing on microstructure and mechanical properties of Ti-6Al-4V TIG weldments, Science and Technology of Welding and Joining 11 (2006) 442-447.

L. Chuan, Z. Jianxun, N. Jing, Numerical and experimental analysis of residual stresses in full-penetration laser beam welding of Ti-6Al-4V alloy, Rare Metal Materials and Engineering 38 (2009) 1317-1320.

P. Ferro, F. Berto. Quantification of the influence of residual stresses on fatigue strength of Al-alloy welded joints by means of the local strain density approach. Strength of Materials 48(3) (2016) 426–436.

P.-H. Chang, T.-L. Teng, Numerical and experimental investigations on the residual stresses of the butt-welded joints, Computational Materials Science 29 (2004) 511-522.

B. Brickstad, B. Josefson, A parametric study of residual stresses in multi-pass butt-welded stainless steel pipes, International Journal of Pressure Vessels and Piping 75 (1998) 11-25.

A.S.H. Kabir, X. Cao, J. Gholipour, P. Wanjara, J. Cuddy, A. Birur, M. Medraj, "Effect of postweld heat treatment on microstructure, hardness, and tensile properties of laser-welded Ti-6Al-4V," Metallurgical and Materials Transactions A, 43 (2012) 4171-4184.

X.-L. Gao, L.-J. Zhang, J. Liu, J.-X. Zhang, "A comparative study of pulsed Nd: YAG laser welding and TIG welding of thin Ti6Al4V titanium alloy plate," Materials Science and Engineering: A, 559 (2013) 14-21.

G. Thomas, V. Ramachandra, R. Ganeshan, R. Vasudevan, "Effect of pre-and post-weld heat treatments on the mechanical properties electron beam welded Ti-6Al-4V alloy," Journal of materials science, 28 (1993) 4892-4899.

P. Dong, S. Song, J. Zhang, "Analysis of residual stress relief mechanisms in post-weld heat treatment," International Journal of Pressure Vessels and Piping, 122 (2014) 6-14.

G. Yan, M. . Tan, A. Crivoi, F. Li, S. Kumar and C.H.N. Chia. Improving the mechanical properties of TIG welding Ti-6Al-4V by post weld heat treatment. Procedia Engineering 207 (2017) 633–638.